ELSEVIER

Journal of Chromatography A, 702 (1995) 3–26

JOURNAL OF CHROMATOGRAPHY A

Review

Separation of biomolecules using adsorptive membranes

D. Keith Roper[a,*], Edwin N. Lightfoot[b]

[a]*Merck Research Laboratories, WP16-121P, Sumneytown Pike, P.O. Box 4, West Point, PA 19486, USA*
[b]*Chemical Engineering Department, University of Wisconsin, 1415 Johnson Drive, Madison, WI 53706, USA*

Abstract

The efficient recovery of labile biomolecules requires rapid, reliable separation processes using mild conditions. Adsorptive membranes are available in a range of chemistries and geometries which permit their application as clarification, concentration, fractionation and purification tools in a biorecovery sequence. Available devices exhibit low backpressure, short residence times and high volumetric throughputs relative to conventional chromatographic packed beds. Non-uniform flow, dead volumes and backmixing observed in some adsorptive membrane systems preclude them from achieving substantial improvements in resolution relative to conventional packed beds. Improvements in design and operation of these systems should increase their separation performance tenfold. Adsorptive separations using affinity, ion-exchange and hydrophobic membranes are reviewed.

Contents

* Corresponding author.

0021-9673/95/$29.00
SSDI 0021-9673(95)00010-0

1. Introduction

The purpose of this review is to examine applications of microporous polymeric membranes as substrates for the adsorptive liquid chromatography of biological macromolecules. Rapid developments in biotechnology and the pharmaceutical potential of biomolecules are fueling demand for reliable, efficient methods to purify preparative amounts of proteins, peptides and nucleic acids. Recombinant gene products currently approved for drug use by the Food and Drug Administration (FDA) include insulin, growth hormone, interferons, erythropoietin and tissue plasminogen activator [1]. Additional polypeptide therapeutics being examined in human clinical trials number in the hundreds; thousands more are currently being investigated.

Recovery of fragile molecules from a biological host environment requires attention to their unique characteristics. For example, time-consuming recovery processes cause unnecessary degradation of many gene products. Variants of proteins and nucleic acids are generated during downstream processing by deamidation, oxidation, proteolysis, nicking and aggregation. The fraction of degradation products increases with residence time [2], so shorter process times can net higher recoveries and product purity.

Mild processing conditions also help to maintain the native conformation and hence the biological activity of biomolecules. Avoiding extreme pH or temperature values, shear and exposure to air–water interfaces prevents subsequent denaturation of many enzymes. Avoiding non-polar solvents and hydrophotic adsorbents which are commonly used to purify small solutes also reduces destabilization of biological products.

Additional considerations arise as biological molecules are prepared in sufficient amounts for evaluation as drug candidates. Selected purification methods must consistently remove potentially hazardous variants, in addition to host cell proteins, DNA, endotoxins and viral elements, from complex feed streams [3]. High resolution is commonly required to meet stringent purification standards set for recombinant DNA products. Variants differing from an enzymatic product by one amino acid or contaminant levels greater than 1 ppm have not been permitted in previous pharmacological preparations [4].

Large-scale recovery operations must be efficient, as the cost of recovering biomolecules can dominate total product manufacturing costs [5]. Inefficient processes consume inordinate volumes of expensive solvents which must eventually be regenerated or disposed. Costs resulting from solvent tankage and consumption during downstream recovery represent a significant fraction of biological recovery costs [6]. Finally, the reliability of process equipment must be well documented to merit approval from regulatory agencies.

These characteristics of biological products and considerations for their preparative recovery are practical issues which are addressed here as we evaluate reported applications of membrane chromatography. The range of reported investigations of membrane adsorption allow us to

consider: (1) what features of adsorptive membranes permit rapid, non-denaturing recovery of biological products?; (2) what is the performance of adsorptive membranes measured using techniques commonly applied to chromatographic packed beds? (3) how are adsorptive membranes best configured and operated to provide adequate resolution and efficiency for biological preparations?

2. Novel chromatographic membranes

Membrane chromatography systems function as short, wide chromatographic columns in which the adsorptive packing consists of one or more microporous membranes in series, each derivatized with adsorptive moieties. They were derived, by and large, from filtration modules and consequently exist in a similar variety of configurations: flat or spiral-wound sheets, hollow fibers and cast cylindrical plugs.

Adsorptive membrane chromatography reflects technological advances in both membrane filtration and fixed-bed liquid chromatography. Membranes are employed as filters to separate biomolecules whose size differs by roughly an order of magnitude or more. Membrane filtration is used in bioprocess recovery to remove cell debris, colloidal or suspended solids [7] and virus particles [8] from homogenized suspensions of bacterial cells. Membranes may be configured in tangential-flow, hollow fiber, asymmetric or dead-end filtration geometries. A recent variation of membrane filtration, called "membrane filtration affinity purification" [9], is intended to increase the selectivity of size-based membrane separations. Affinity ligands are coupled to nanoparticles in order to bind selectively proteins of interest. The particles are subsequently filtered from the process stream.

By comparison, separation occurs in liquid chromatography as molecules in a mobile stream are preferentially retained by an adjacent stationary phase. Less strongly retained molecules are carried away by the solvent stream, gradually leaving a pure band of the preferentially adsorbed species. To increase the chromatographic capacity, ligands specific to the retained species are bound to the large, intraparticle surface area of porous resins. Mobile phase species access these ligands by Brownian thermal diffusion.

Chemical modification of filtration membranes to adsorb biomolecules in the filtrate originally employed biospecific affinity ligands [10]. Dissolved molecules are carried directly to adsorptive sites in these membranes by bulk flow, eliminating the long diffusion time required by resin-based chromatography. This adaptation increases the throughput of affinity processes. Ligands intended for pseudo-affinity, ion-exchange, hydrophobic interaction and reversed-phased interaction have also been coupled to membrane substrates.

Many adsorptive membrane separations are performed using conventional filtration apparatus to concentrate and recover the product of interest. Other adsorptive membranes are configured for compatibility with existing chromatographic pumps, detectors and associated peripherals. The term "high-performance membrane chromatography" has been applied to separations achieved by selective adsorption or retention on membrane substrates [11,12].

3. Scope of the review

The literature which describes column liquid chromatography or membrane filtration is large and comprehensive. The scope of this review is limited to analyses and applications of adsorptive membrane systems, which are the hybrid synthesis of these two technologies. Adsorptive membranes are being applied to separations in many fields. We review representative applications, paying particular attention to work whose scope indicates features peculiar to adsorptive membranes, or suggests developments in their design and operation. It will become apparent that an understanding of fundamental chromatographic principles is useful in order to take advantage of the unique attributes of membranes as adsorptive substrates. Advances in the sciences of membrane filtration and column chro-

matography are also likely to improve membrane chromatography.

4. Adsorptive membrane chromatography

Adsorptive membranes consist of a substrate to which an interactive ligand is chemically coupled. These membrane systems are available for use in a number of separation configurations or geometries. We review in Section 4.1 reported substrates and coupling chemistries. We then consider in Section 4.2 a variety of separation configurations and briefly discuss the applications for which they appear best suited. We conclude in Section 4.3 with a summary of available adsorptive membrane systems whose performance has been characterized.

4.1. Membrane substrates and coupling chemistries

Ideally, adsorptive membrane substrates are mechanically resilient and resistant to solvents used to activate coupling [10]. They should not participate in secondary hydrophobic adsorption. Hydrophobic adsorption produces non-specific retention that interferes with product resolution and can also contribute to the denaturation of biopolymers. Polymeric and inorganic materials which constitute membrane substrates in several different geometries are listed in Table 1. Many of these materials are also widely used as membrane filters.

Cellulose is a popular substrate for adsorptive membranes. Native and derivatized cellulose membranes are soluble only in some strong acids [10]. Ion-exchange activity of residual carboxylic and aldehyde side groups can be neutralized with borohydride reduction, and secondary hydrophobic interactions are eliminated by the high level of hydration in these membranes. Rigid, hydrophilic cellulose grafted with gel-type polymers has been linked to spacer arms on which active derivatives for ligand coupling were introduced [13]. Regenerated cellulose is non-rigid and must be adequately supported to prevent deformation or wrinkling.

Several recent investigators have examined adsorptive membranes made of acrylic copolymers. Thin discs of macroporous poly(glycidyl methacrylate–co-ethylene dimethacrylate) (GMA–EDMA) have been synthesized by free-radical polymerization of a mixture of a monovinyl monomer, such as styrene or methacrylate, and a divinyl monomer such as divinylbenzene, in a heated mold [11,14]. Synthesis is initiated by azobisisobutyronitrile in the presence of porogenic solvents between two heated plates. Epoxy groups are modified to furnish functional group sites for hydrophobic interaction chromatography (HIC) or ion-exchange chromatography (IEC). Sulfuric acid hydrolysis destroys residual underivatized groups to prevent secon-

Table 1
Common geometries and materials of chromatographic membranes

Geometry	Material	Ref.
Thin sheet	Cellulose	[13]
	Regenerated cellulose	[31,40]
	Poly(glycidyl methacrylate–co-ethylene dimethacrylate)	[15,14,11]
	Poly(glycidyl methacrylate)	[16]
	Nylon	[39]
	Titanium	[19]
Hollow fiber	Polyethlyene	[22]
	Silicon dioxide glass	[24]
Spiral-wound	Cellulose/GMA–DEAEMA copolymer	[73]
Cross-linked rod	Poly(styrene–co-divinylbenzene)	[17,18]

dary associations between biomolecules and the substrate [15]. A GMA substrate is also commercially available [16].

A reported polymerization similar to that for GMA–EDMA has been used to synthesize a continuous rod of microporous, membrane-like substrate directly within a cylindrical column [17,18]. The poly(styrene–co-divinvylbenzene) matrix was used directly for reversed-phase chromatography of model polypeptides and proteins. Polymer rods fill the void volume corresponding to interstitial pore spaces characteristic of granular packed beds with additional porous substrate. The minimum interstitial, non-adsorptive dead volume in a bed packed with cylindrical spheres was estimated to be 26%. Nylon substrates are also used.

In addition to polymers, inorganic substrates have been studied. An ion-exchange membrane has been formed using an oxide of titanium. Polyethyleneimine (PEI) ion-paired with the oxide support and was subsequently cross-linked with glutaraldehyde to form a reactive film to which anion-exchange ligands were coupled [19]. Titania is more alkali stable than silica, and adsorption of PEI on titania is straightforward [20]. Alkaline conditions will not erode the PEI coating.

Unlike flat membrane sheets which are typically supported in conventional filtration apparatus, hollow-fiber membranes must be intrinsically rigid, as well as hydrophic and resistant to solvents. Adsorptive membrane hollow fibers formed from both polymeric and inorganic substrates have been examined.

Radiation-induced graft polymerization of 2-hydroxyethyl methacrylate (HEMA), vinyl acetate (VAc) and glycidyl methacrylate (GMA) on to a polyethylene hollow-fiber microfiltration membrane introduced alchoholic hydroxyl groups that reduced non-selective protein adsorption in proportion to diol density while maintaining pure water flux [21]. Protein binding changed from irreversible to reversible. The hydrophilized membrane served as a microporous support on to which sulfopropyl groups were immobilized for the anion exchange of lysozyme.

Two affinity systems have also been produced by coupling with the epoxide groups of GMA. A hydrophobic amino acid, L-phenylalanine, was coupled to form a pseudo-biospecific ligand for selective immobilization of bovine γ-globulin [22]. Chemical conversion of the expoxide to iminodiacetate and subsequent chelation with copper were used to produce an immobilized metal affinity membrane (IMAM) [23]. As with the thin-sheet disks, sulfuric acid treatment of unconverted epoxide reduced non-specific adsorption by His–Leu and bovine serum albumin (BSA). Glass hollow-fiber microfiltration membranes have also been used as substrates for immobilized metal chelate affinity membranes [24].

Commercially available substrates and coupling chemistries are available in addition to those we have considered. Protein A and IgG were coupled to epoxy-activated polymeric membranes by 16 h of incubation at an optimum pH of about 8 [25]. Remaining reactive groups were blocked by treatment with 2% ethyl glycinate in 0.1 *M* borate bufer. Ligands including plant lectins, carbohydrates and enzyme inhibitors can be attached to monoclonal antibodies using a stable secondary amine linkage which allows little leaching.

We now consider the relative merits of each of the geometries of membrane chromatography.

4.2. Adsorptive membrane geometry

Adsorptive membrane chromatography can be performed using a number of commercially available or laboratory-prepared geometries. In Fig. 1 we illustrate individual thin-sheet and hollow-fiber membranes together with stacked-membrane, spiral-wound and Chromarod membrane columns.

Individual membranes in the form of thin sheets, disks or hollow fibers are convenient inexpensive and versatile. Sheets or disks may be mounted in conventional ultrafiltration units or in specially prepared cartridges. This permits rapid, low-pressure adsorption of limited amounts of sorbate, in either batch or continuous recycle mode. In this way, intended product may be concentrated substantially. Individual

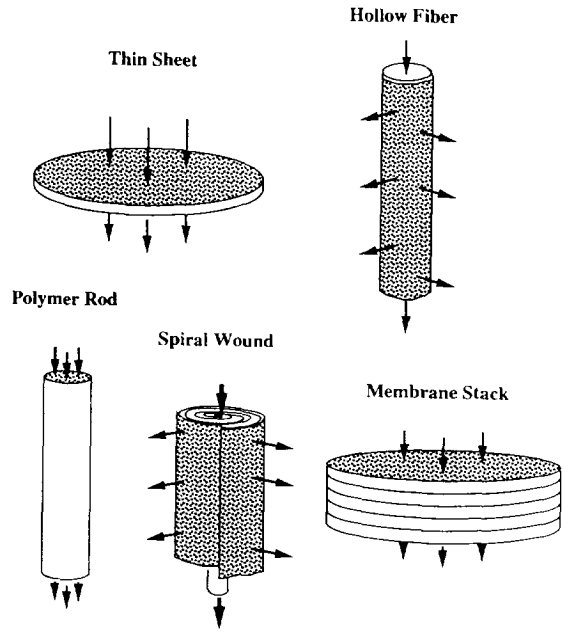

Fig. 1. Schematic comparison of the configurations that have been proposed for membrane-based adsorption. Arrows illustrate the direction(s) of bulk flow. Pattern indicates membrane cross-sectional area which lies roughly perpendicular to bulk flow.

sheets or disks appear best suited for laboratory methods which selectively adsorb the product of interest from a large, dilute sample volume.

Product recovery from complex feed volumes such as homogenized cell paste, animal serum or blood plasma typically fouls dead-end adsorption systems. High-molecular mass antifoams added to fermentation broths also foul membranes and can reduce flux rates by 50% or more [26]. Cross-flow operation utilizing either sheets or hollow fibers has been used to treat such feeds at small scale [27]. Hollow fibers are usually available bundled within a shell using potting material that may swell if exposed to organic solvents.

The capacity of single adsorptive membranes for preparative recovery may be limited. To achieve the adsorptive capacities necessary for preparative biological recovery, multiple thin-sheet disk membranes are stacked in series and housed in a rigid cylindrical shell. Alternatively, a single thin sheet wound around a permeable, cylindrical core can be similarly packaged. Stacked-membrane and spiral-wound geometries allow local variations in porosity and membrane thickness which may compromise the separation performance of single sheets [28] to be averaged out in the direction of flow.

Adsorptive spiral-wound and stacked membrane columns are compatible with conventional high-performance liquid chromatography (HPLC) systems. They have a number of advantages relative to packed-bed chromatography. The cross-sectional dimension of membrane columns which lies perpendicular to the flow direction is considerably longer than the flow path. In contrast, granular adsorptive beds are commonly packed with a length-to-diameter ratio of 2.5 or greater. The large packed-column aspect ratio is necessary to maintain frictional support to resins from the column wall, in order to resist settling and cracking [29]. Consequently, membrane-column residence times are short and backpressures are small, whereas the volumetric capacity is large with respect to large-scale chromatography [30]. These features increase throughput and decrease processing times, as discussed in Section 6, reducing the requirement for expensive or hazardous solvents and tankage. They also yield shorter residence times, which in turn reduces protein degradation by proteolysis and denaturation. Fig. 2 contrasts stacked-membrane and resin-packed columns.

Despite their abbreviated flow path, adsorptive membrane columns achieve resolutions comparable to those with packed chromatographic beds [31]. Separation performance of membrane chromatography is considered further in Section 5. On the other hand, it has been reported that the shallow flow path of spiral-wound adsorptive beds precludes high-resolution separations [13]. In spiral-wound membranes the flow direction does not coincide with gravity. Small defects are not self-stabilized by radial flow through the bed. This potentially biases spiral-wound beds toward channeling.

Membrane rod chromatography by Svec [17,18] produces a column with attributes of both membrane adsorbers and packed resin beds. Like an adsorptive membrane, the polymeric

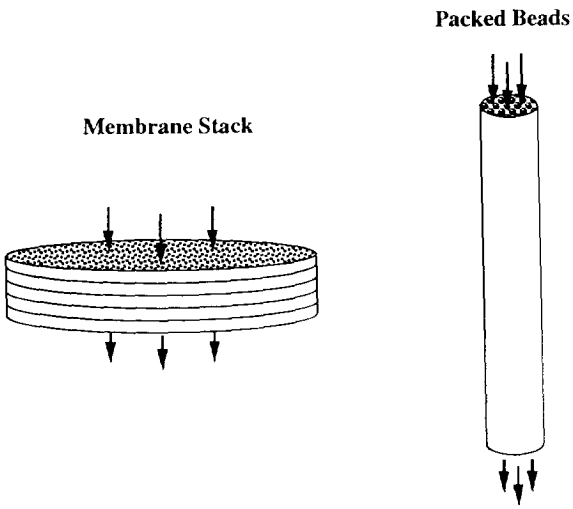

Fig. 2. Comparison of membrane stack with packed bed for adsorptive chromatography. Hold-up volumes of both systems are similar. Length-to-width aspect ratio of packed bed often corresponds to width-to-length dimensions of stacked membrane. This results in lower backpressures and larger volumetric throughput for stacked membranes.

matrix of the cylindrical plug cast within a column is a macroporous structure (0.1–10.0 μm I.D.) producing relatively low backpressure. Linear decreases in efficiency due to intraparticle diffusion at increasing flow-rates are not observed. Channeling or settling is unexpected in the matrix. At the same time, the matrix is resistant to deformation, like a packed resin bed, and column length-to-width aspect ratios are well above 2.5.

4.3. *Membrane chromatographic columns*

A number of commercially available adsorptive membrane devices have been considered in the literature. Many of these are summarized with their respective manufacturers and categorized by type of interactive chemistry or activity in Table 2.

Ion-exchange membranes and their manufacturers include Millipore MemSep, LKB Zeta Prep and FMC ActiDisc and Acti-Mod cartridge, Amicon MAC capsules, Sartorius Sartobind Q and S and Pall Lowprodyne membranes. Apparently the earliest commercially available ion-exchange membrane was a cation-exchange disk, SP-Zetaprep from LKB, (Bromma Sweden) [72]. Affinity systems consisting of protein A and protein G ligated to cellulose are available (Millipore MemSep; Memtek MAC disks, Genex AbSorbent G and Cuno Zetaffinity).

Table 2
Commercially available adsorptive membranes whose performance has been previously examined

Tradename	Type	Manufacturer	Ref.
MAC	Anion exchange	Amicon Division (Memtek), W.R. Grace, Beverly, MA, USA	[59]
Zetaffinity 10	Affinity	Cuno, Life Sciences, CT, USA	[13]
ActiDisc, Acti-Mod	DEAE	FMC Bioproducts, Rockland, ME, USA	[14,59]
Quick Disk	Q, C-4	Säulentechnik Knauer, Berlin, Germany	[16]
AbSorbent	Protein G	Genex	[38]
MemSep	DEAE, QMA, SP, protein A and G	Millipore, Bedford, MA, USA	[31,47,60]
Loprodyne	Protein A	Pall Bio Support, Portsmouth, UK	[30,39]
Sartobind	Q, S Epoxy	Sartorius	[25,42,53]
Zetaprep	SP	LKB, Bromma, Sweden	[54,72]

Morphologies different than conventional stacked beds include radial flow through spiral-wound cartridges, such as the ion-exchange ZetaPrep cartridges and affinity Zetaffinity 10 cartridges.

5. Adsorptive membrane chromatographic performance

The separation effectiveness in adsorptive membrane chromatography increases with the number of available adsorptive sites and their relative affinity for the biological molecule of interest. Separation efficiency decreases owing to backmixing, dispersion, molecular diffusion and finite ligand–ligate association rates.

5.1. Characterizing membrane columns

The separation performance and physical attributes of adsorptive membrane units are characterized in much the same fashion as chromatographic packed beds. Most commonly, the effluent response to a sharp input pulse or step change in concentration of a single model adsorbate is detected using UV–Vis absorption. Features of the curve, notably its temporal moments, indirectly indicate mass transport rate effects such as dispersion, backmixing and ligand–ligate interactions. They are also used to measure equilibrium adsorption attributes which include column capacity and non-linear interaction at high adsorbate concentration.

Recently, environmental scanning electron microscopy [32] and nuclear magnetic resonance microscopy [33] have been used to characterize membrane separchim units in order to avoid the ambiguities associated with effluent analysis. Both are high-resolution techniques. Magnetic resonance has the advantage of allowing non-destructive and non-invasive visualization of static and operating units using one of a number of contrast sensitivities [34,35].

A magnetic resonance image of a representative adsorptive stacked membrane, the MemSep 1000 cartridge (Millipore, Bedford, MA USA) is reproduced in Fig. 3 [36]. The dimensions of the

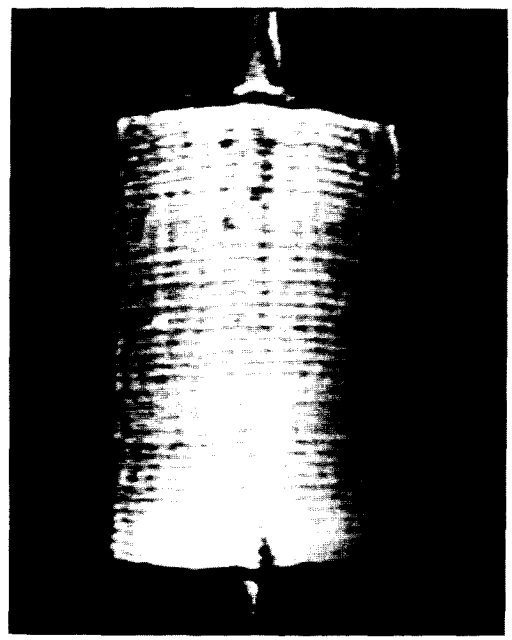

Fig. 3. Spin-echo magnetic resonance image of an adsorptive stacked membrane. A 1.8-mm sagittal slice parallel to the axis and through the centerline of a MemSep 1000 is shown. The cartridge is connected to inlet and outlet tubing and filled with non-flowing water. A long spin–lattice relaxation delay (1 s) and short spin–spin relaxation delay (0.4 ms) make signal intensity or brightness proportional to proton density. The length-to-width aspect ratio of the membrane bed in the image, 1.2:1, is six times larger than the physical ratio of 1:5 to enlarge physical features of the adsorptive bed.

stacked-membrane bed are 5 mm × 17.17 mm I.D., which constitutes a 1.4-ml nominal bed volume. The length-to-width aspect ratio of the cartridge which appears in the image (1.2:1) is six times larger than the actual ratio (1:5) in order to enlarge physical features of the adsorptive bed. Forty microporous membranes approximately 120 μm thick with a nominal pore diameter of 1.2 μm comprise the stack. The membrane substrate is pure regenerated cellulose. A uniform matrix porosity of 0.827 has been reported [37].

The spin-echo image in Fig. 3 illustrates water distributed in a 1-mm slice of a MemSep 1000 stacked membrane parallel to its axis and through its centerline. Signal intensity (white-

ness) is proportional to proton density or water concentration. Incoming mobile solvent (white) enters the column by passing through an upstream Luer-lock adaptor (top). Porous frits (black) at upstream and downstream ends of the membrane bed (grayish to white) distribute incoming fluid across the membrane cross-sectional area. (The frits appear bowed owing, in part, to the contracted horizontal aspect of the image.) Nine donut-shaped gaskets (black), which appear as rectangles on either side of the bed, encircle the stack, separating every four membranes. They are intended to exclude solvent from the bed periphery and prevent incoming fluid from bypassing membrane stack. Outgoing solvent (white) leaves the column through a thin Luer-lock adaptor.

5.2. Mass transport effectiveness

Dissolved solute molecules are transported through an adsorptive membrane by bulk flow of the mobile solvent (convection). Within the membrane, solutes experience three consecutive transport rate resistances to ideal, equilibrium separation: dispersion, Brownian thermal diffusion and kinetic sorbate–sorbent interaction. We briefly consider each of these processes in succession. A pictorial representation of convection and dispersion at the microscopic level is suggested in Fig. 4.

5.2.1. Convection

At a pseudo-continuum scale large with respect to membrane porosity, but small relative to membrane dimensions, bulk flow through porous membranes has been characterized by Darcy's law with a membrane permeability given by the Blake–Kozeny equation [11]. In this description, local velocity is proportional to local pressure drop, as has been demonstrated [30]. GMA–EDMA copolymer membranes exhibited a linear increase in permeability with increasing pressure drop [38]. Nominal pore sizes reported for two nylon membranes, 0.45 and 3 μm, are representative of the range of pore diameters found in adsorptive membranes [39]. Measured permeability of the 3-μm membrane was ten times

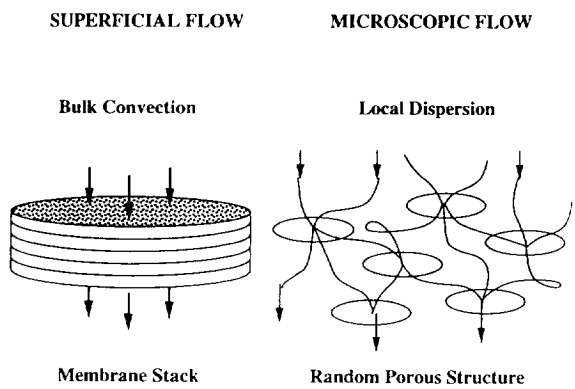

Fig. 4. Idealized diagram showing bulk flow of solvent through a membrane stack and microscopic dispersion of solvent within membranes pores. Characteristic mass transport effects differ at different scales. The random porous structure in adsorptive membranes, whose nominal dimension is of the order of microns, exhibits local mixing. Stacked-membrane beds, whose dimensions are of the order of millimeters, exhibit pressure-dependent flow.

that of the 0.45-μm sheet. Polymer-rod columns have an average pore size of 19.5 μm [18].

Ideally, bulk flow of solvent carries adsorbate molecules toward the column outlet at the same rate in each volume of the column. Accordingly, physical and mathematical descriptions of packed-bed chromatography generally assume a constant, uniform interstitial velocity. In adsorptive membranes, however, it has been shown that the axially directed velocity of a mobile solvent can be much faster in the center of the separation unit than near the edges of the adsorptive bed. Direct, *in situ* measurements of local velocity in operating membrane separation units obtained by magnetic resonance flow imaging reveal non-uniform radial and axial variations in interstitial velocity [40]. The decrease in apparent porosity from the center of the bed to the gasket area evident in Fig. 3 may account for the decrease in velocity observed adjacent to the gaskets. Velocity in ideal porous media increases non-linearly with void fraction [41]. Jetting occurs around the center of another membrane stack at flow-rates exceeding 5 ml/min, resulting in little or no adsorption near the periphery [42].

Bypassing and uneven fluid distribution are additional sources of non-uniform flow. Incom-

ing fluid which bypasses the membrane stack or distributes unevenly across the adsorptive membrane cross-section has been indirectly observed by dye injection [14]. Other stacked-membrane systems, however, have demonstrated an absence of bypassing or channeling [43]. A fluid distributor consisting of semicircular channels radiating out from the fluid inlet which were connected by annular grooves gave the most even fluid distribution in a group of laboratory-scale stacked-membrane columns [14].

Where they are present, local variations in the rate of bulk flow within a column degrade a separation by backmixing previously separated solutes. The result is asymmetric elution peaks and breakthrough curves with unexpected width. The most pervasive indication of non-uniform flow in membrane systems is peak tailing. Tailing is pronounced in peaks from step-gradient elution of model proteins from adsorptive membranes [11,42,43]. Illustrated effluent profiles from a variety of commercially available stacked-membrane columns exhibit notable tailing [16,25,44]. Secondary solute–matrix interactions could also contribute to tailing of eluting peaks.

The most direct evidence linking tailing and non-uniform flow combines magnetic resonance flow imaging, effluent analysis and a novel reversed-flow experiment to descriminate between tailing due to extra-column dispersion and tailing due to non-uniform flow using a non-adsorptive tracer [40]. Quantitative decreases in separation efficiency corresponding to asymmetry and especially peak tailing in effluent responses from non-adsorbing pulse injections have been linked directly to non-uniform flow.

5.2.2. Dispersion

During convection in bulk flow, individual adsorbate molecules are dispersed owing to micro-scale fluid-phase phenomena [45]: mixing by solid obstructions to flow, incomplete connectivity, eddies and recirculation from regional pressure gradients. An analytical description of Fickian convective dispersion also includes the dispersive effect of random Brownian diffusion in the direction of flow [46].

In the absence of backmixing and intraparticle diffusion, convective dispersion remains as the primary contributor to band broadening or separation inefficiency in adsorptive membranes. Broadening due to dispersion can be estimated by analogy with packed chromatographic beds [47]. Widths of effluent profiles from adsorptive membranes broadened by dispersion alone are expected to decrease with increasing velocity, giving plate heights on the order of 1 μm.

5.2.3. Diffusion

The primary mass transport advantage of adsorptive membranes relative to conventional packed beds is their lack of intraparticle diffusion. To access most of the adsorptive capacity in a packed bed, adsorbates must diffuse from the flowing, interstitial fluid through tortuous, porous particles. Hence the effective path length for intraparticle diffusion in conventional chromatography corresponds to the particle diameter, which typically exceeds 5–10 μm on the preparative scale owing to backpressure limitations. In derivatized membranes, adsorptive sites are directly adjacent to the bulk fluid, so the effective diffusion path length is less than the substrate pore size, which, in turn, is commonly less than 1 μm. Increasing the membrane pore size from 0.45 to 3 μm had no measurable effect on the adsorption rate [39], suggesting solutes were quickly convected to adsorption sites on membrane surfaces.

Reducing the diffusional path length allows volumetric throughputs to be increased substantially, while maintaining membrane capacity. A reduction in intraparticle diffusion noted for macroporous, pellicular resins affords a similar advantage [48]. Adsorption efficiency is increased dramatically for biological macromolecules such as proteins and plasmid DNA, since the diffusion rate is proportional to solute diffusivity.

Nonetheless, diffusion of adsorbates into other dead volumes which are permeated by the mobile phase but inaccessible to flow could affect the separation efficiency and prolong regeneration. For example, the presence of a signal between adjacent exclusion gaskets in Fig. 3 (about 0.25 mm apart) implies that these vol-

umes are accessible to buffers and dissolved solutes by Fickian diffusion. An order-of-magnitude estimate of the diffusive solute permeation distance into the gap between gaskets is $L = (2DT_\nu)^{1/2}$, where T_ν is the permeation time-scale and D and ν are solute diffusivity and interstitial velocity, respectively.

For slow (1 ml/min), narrow-pulse protein separations typical of chromatographic analysis, the appropriate permeation time-scale is $0.25/\nu$, which equals the 0.25 mm separating the gaskets divided by the solute velocity past the gap. This shows that the corresponding distance is negligible (about 1 μm). However, for adsorptive membrane concentration in preparative bioseparations using frontal or recirculating operating modes, the time available for permeation may be 1 h or more. The corresponding permeation distance approaches 100 μm. Complete recovery of product that diffused between gaskets will take at least as long as the initial loading. It has been observed experimentally that about 2 h are necessary to exchange buffers completely and achieve a steady UV absorbance baseline in a MemSep 1000 [40]. This equilibration time corresponds to the time required for a salt to diffuse from the stacked-membrane periphery, through the intergasket gap to the moving fluid phase.

5.2.4. Adsorption

The rate of adsorption on to conventional ion-exchange and hydrophobic interaction media is typically unappreciable with respect to dispersive and diffusional resistances to mass transport. Sorbate–sorbent interaction is often considered instantaneous [39]. On the other hand, the formation of an affinity complex is often so slow as to become the rate-limiting mass transport process [49]. It remains to be shown that convective dispersion is negligible with respect to reaction kinetics in existing affinity membrane systems. Affinity association kinetics must be considered in determining the operating velocity of a membrane which optimizes dynamic capacity.

5.2.5. Extra-column backmixing

The separation performance of adsorptive membranes can be severely degraded by backmixing in volumes outside the adsorptive membrane bed: distributors, tubing, adaptors, valves, mixers and pumps. Excessive peak broadening and dilution have been attributed to significant dead volumes in fluid distributors [14], filter holders [50] and Luer slip outlets [42]. The last appeared to act as a continuous mixer. A 1-ml extra-column void volume, monitored by UV adsorption of effluent BSA in a non-adsorbing mobile phase, produced a broad, asymmetric breakthrough curve under adsorbing conditions [51]. This broadened transitions between plateaus of emerging eluents which have differing binding affinities.

Extra-column band broadening is more significant in adsorptive membrane systems than in chromatographic columns owing to the large ratio of throughput to bed volume in the former. Experimental evidence suggests that extra-column band broadening changes little with velocity [52]. Its effect is significant relative to other mass transport resistances, and has been observed to predominate [51].

A simple experimental protocol has been suggested to discriminate between peak broadening and tailing arising from extra-column backmixing, convective dispersion or non-uniform flow [47]. This should allow users to select a membrane stack with the highest separation potential, and allow manufacturers to design more efficient membrane adsorption systems.

5.3. Thermodynamics of adsorptive membranes

Having accounted for the possible degradation of separation efficiency of backmixing and resistance to mass transport, we now consider the intrinsic separation potential of membranes determined by the available number of adsorptive sites and their relative affinity for the molecule of interest. We discuss measured capacities of adsorptive membranes and measurements and models of their equilibrium behavior.

5.3.1. Capacity

Reported capacities for several adsorptive membranes are summarized in Table 3. Static capacities increased from 3.3 to just over 50 mg

Table 3
Reported capacity values of adsorptive membranes for several biological macromolecules: monoclonal antibody (MAb), malate dehydrogenase (Md), human serum albumin (HSA), ribonuclease (Rib), lysozyme (Lys), ovalbumin (Ova), bovine serum albumin (BSA), γ-globulin (G-G), immunglobulin G (IgG) and a mixture of IgG and IgA (BGG)

Membrane	Capacity (g/m^2)	Static capacity (mg/ml)	Dynamic capacity (mg/ml)	Ref.
C-4		200–400	50	[38]
Cation exchange			50 (MAb)	[55]
Dye affinity	10.7 (Md)	50.8 (Md)	45.7 (Md)	[53]
Anion exchange			5.8 (HSA)	[31]
Copolymer		20 (Rib), 26 (Lys), 47 (Ova)	5 (Rib), 0 (Lys), 5 (Ova)	[38]
Copolymer		40 (Ova)		[15]
L-Phe affinity hollow fiber			50 mg BGG/g fiber	[22]
Anion exchange			30–40 g BSA/g membrane	[16]
Anion exchange	1.29	20		[19]
Dye affinity		8.6 (Lys), 5.6 (BSA)	7.8 (Lys), 7.6 (BSA)	[57]
Protein A/ IgG affinity		4.74 (IgG–rabbit), 0.51 (protein A)		[25]
Protein A affinity		3.3 (G-G)	2.9 (G-G)	[39]
Ion exchange			8 IgG per cartridge	[54]

macromolecule per ml of membrane. These are typically lower than for comparable porous chromatographic resins, with occasional exceptions [30]. It has been reported that the volumetric capacity is large with respect to large-scale chromatography [30].

Static capacity values are obtained by equilibrating a known amount of membrane with a concentrated volume of dissolved solute and measuring the solute uptake relative to the membrane volume. Mass, volume and surface-area measurements which are equivalent are unique to each membrane and allow capacity to be expressed in alternative units. For example, 1 cm^2 of Sartobind Blue 2 membrane corresponds to 0.021 ml or 8.2 mg of the membrane [53].

Dynamic capacity values are obtained by flowing concentrated solute through a membrane and measuring the mass adsorbed per unit volume of membrane bed at a breakthrough concentration 10% of the inlet concentration [50]. Some adsorbent volumes remain unused owing to back-mixing, non-uniform flow and resistance from mass transport rate processes. As a result, dynamic capacities are smaller than corresponding static values. Solute capacity varies with adsorptive conditions including solvent composition, buffer concentration, pH and flow-rate [54]. Increasing the flow-rate lowered membrane capacities in the ion exchange of selected model proteins, while slightly raising the hydrophobic interaction capacity in other systems [11,42]. A dynamic capacity of 50 mg/ml for MAb on a strongly acidic S cation exchanger was obtained

while loading of flow-rates exceeding 800 ml/min (0.57 cm/min) on a pleated 1400 cm^2 membrane [55].

The dynamic capacity of one dye-affinity membrane remained within 95% of its static value, whereas that of a corresponding dye-affinity packed bed decreased by 50% when linear velocity was increased over tenfold [54]. The column however, retained more of its original capacity as the percentage of *Escherichia coli* extract added to the feed was increased to 10%, while the membrane became blocked at 5%. Dynamic capacities were also maintained after more than ten-fold flow-rate increases for HSA adsorption on a DEAE anion exchanger [31].

The capacity of a protein A membrane decreased by 30% after about 30 use and regeneration cycles, suggesting that its long-term stability may be suspect [25]. In general, affinity matrices containing proteins cannot be cleaned with NaOH or used with high protein concentrations or crude solutions. In contrast, binding capacities in ion-exchange membranes are routinely maintained after 25–100 cycles of use and high-salt regeneration [42,56].

Membrane geometry and coupling chemistry also influence capacity. The measured capacity of Ultipor microfiltration membranes was highest when PEI was used as a spacer arm to couple Cibacron Blue F3G-A to the nylon-66 membrane substrate [57]. In nylon membranes with 0.45- and 3-μm pores, the static and dynamic capacities were 3.3 and 2.9 mg/ml, respectively, for membranes [39].

This suggests using the membrane with the larger pore size to decrease the backpressure at higher flow-rates.

5.3.2. Equilibrium

Measured adsorption equilibrium isotherms of protein A, IgG [25] and BSA [30] on pseudo-affinity membranes appear to be of the Langmuir type. This suggests that an adsorption monolayer exists and that non-linear effects on separation performance at high surface concentrations of adsorbate are significant. Values of Z (the number of interaction sites for a solute–adsorbent pair) and log K (parameter including equilibrium formation constant, phase ratio and bound solute concentration) obtained experimentally for ion-exchange adsorptive membranes are smaller than under comparable packed-bed conditions [11]. Local equilibrium behavior of multi-component adsorption has been observed on ion exchangers [58]. The sum of the natural logarithms of the retention and capacity factors on reversed-phase polymer rods decreased in proportion to the organic volume fraction [18]. This is comparable to reported reversed-phase packed-bed behavior.

Single and binary solute adsorption on affinity membranes has been theoretically analyzed using a local-equilibrium model [59]. Computer simulations indicated that solutes with identical equilibrium sorption isotherms whose sorption kinetics differ can be separated on affinity membranes. Simulated axial diffusion and slow adsorption degrade separation owing to differences in local equilibrium, particularly on membrane stacks less than 3 cm. Local equilibrium behavior is not reached on commercially available units at typical operating flow-rates.

Adsorption-rate models of membranes which fail to account for the effects of non-uniform flow, convective dispersion and extra-column broadening which dominate adsorptive membrane mass transport (see Section 5.2) cannot be expected to predict reliably effluent shape or describe separation performance.

5.4. Plate height estimates of membrane efficiency

A popular, scale-independent measure of adsorptive separation efficiency is the plate height, H, or column height equivalent to a theoretical plate. For systems with a linear adsorption isotherm, constant equilibrium distribution coefficient, concentration-independent transport properties and uniform flow, the plate height is defined as the ratio of effluent peak variance to the length of the column. The plate height decreases with increasing column efficiency.

A description of separation efficiency in adsorptive membranes based on fundamental mass transport processes suggests that plate heights should decrease from about 10 μm at 0.05 cm/

min to less than 1 μm at about 5 cm/min [33]. Corresponding plate height measurements in two membrane columns in the absence of non-uniform flow and extra-column backmixing agreed with this description. Reported plate height and corresponding velocity ranges for membrane adsorbers are summarized in Table 4.

Reported plate height estimates vary over three orders of magnitude in the same range of velocity. Other than for a single, 200-μm membrane supported in an ultrafiltration cell [25], the remaining plate heights were estimated for stacked-membrane cartridges. Varying plate height estimation methods, unaccounted for backmixing and variations in stacked-membrane structure and operation contributed to the range of reported values.

Investigators in four studies observed significant increases in effluent band broadening (and therefore plate height) due to dispersion in extra-column dead volumes [57,25,52,47]. However, in only two cases were extra-column effects removed from plate height estimates. Extra-column broadening is probably the reason for the unexpectedly large reported plate heights and their relatively small increase with velocity.

The theoretically large efficiencies of membrane adsorbers are not realized in most reported separations. Measured plate heights, for the most part, have been comparable to fixed-bed efficiencies [60]. At the same time, few mixtures of model proteins require more than a handful of theoretical plates to achieve a product purity in excess of 98% [61].

6. Operation of membrane adsorption

Building on experimental results which illustrate their unique mass transport, thermodynamic and geometrical aspects, we summarize the appropriate operation of adsorptive membranes.

In Section 6.1 we review the location within a biological recovery sequence appropriate for membrane adsorption. We then consider in Section 6.2 operating modes of membrane adsorption. In Section 6.3 the reported throughput of membrane adsorption is compared with that of conventional packed-bed chromatography.

6.1. Membrane adsorption in biological recovery

Recovery of labile genetic templates or gene products for their biological host environment typically involves several consecutive isolation processes which distinguish the product from one or more contaminants based their differing physico-chemical structures. It is useful to organize the individual processes of a non-denaturing, protein recovery sequence into four categories as suggested by Scopes [62] and Lightfoot and Cockrem [63]. A cellular extract, harvested from the fermentation, which contains unexcreted product is first homegenized and clarified to render the product accessible. Lysis of whole cells by enzymatic degradation, ultrasonication, Gaulin-press homogenization or milling releases

Table 4
Experimental adsorptive membrane plate heights (H)

H range (μm)	Velocity range (cm/min)	Estimation method	Extra-column mixing included	Ref.
3.3–0.59	0.52–3.8	Reversed-flow	No	[47]
3–7	0.07–0.22	Unreported	Yes	[25]
25	0.1–2	Unreported		[31]
50–110	4–1.5	EMG fit	Yes	[44]
80–160	1–45	Unreported		[18]
400	0.04–1	Unreported	Yes	[11]
250–800	0.035–6.5	Moments	No	[52]

and solubilizes intracellular enzymes. Subsequent precipitation of cell debris, nucleic acids and insoluble proteins by centrifugation decreases fouling in later process steps. Selective precipitation is effected by adding salt, organic solvent, detergent or polymers such as polyethyleneimine and poly(ethylene glycol) to the buffered cell lysate [64].

Size-selective membrane microfiltration removes cell debris, colloidal or suspended solids or virus particles [8] from the clarified lysate. Subsequent diafiltration into an appropriate buffer prepares the solution for a concentrating adsorptive process in an economical fashion [26]. Microfiltration and concentration have been performed simultaneously using a spiral-wound membrane adsorber [54]. Incompletely clarified lysate has been shown to foul dead-end stacked-membrane adsorbers, at concentrations as low as 5% [53]. Membrane adsorption has also been applied simultaneously to filter and concentrate recombinant product secreted into a complex fermentation medium. Elution of the bioproduct and contaminants with similar physical properties is discussed in Section 6.2.

Additional complementary separation processes are usually required to fractionate the product from similar contaminants based on differences in size, mass, isoelectric point, charge density and hydrophobicity. Examples of affinity, ion-exchange, hydrophobic interaction and reversed-phase membrane adsorbers used to fractionate product mixtures are discussed in Section 7.

Finally, the concentrated product is purified from closely related variants by a high-resolution technique (prior to final formulation and packaging of pharmaceutical bioproducts). Purification often requires differential adsorption in an adsorptive column with a large number of theoretical plates to attain the required purity. Overall recovery yields which had hovered at about 30% are becoming as high as 60–70% in recent reports [65].

In Fig. 5 the consecutive isolation processes are shown. Adsorptive membranes have been inserted in the clarification, concentration, fractionation and purification steps. In these processes, literature reports have indicated their successful application in a similar recovery train.

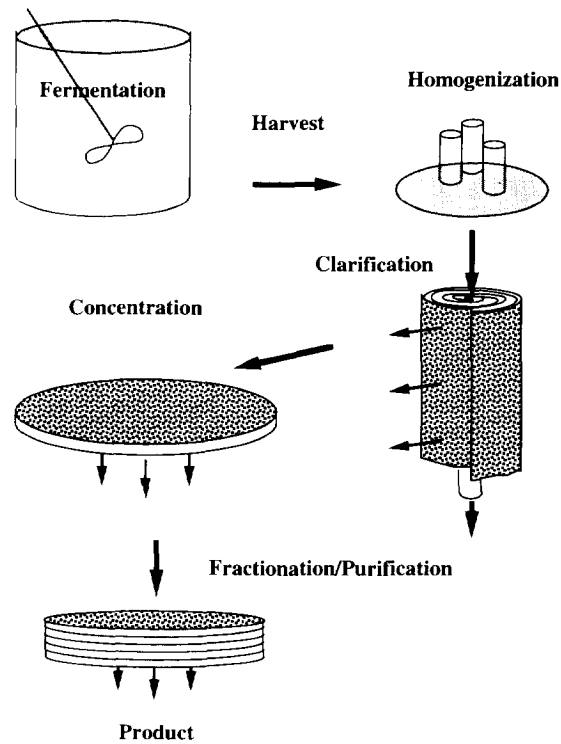

Fig. 5. Schematic illustration showing a typical sequence of processes to recover non-secreted protein from bacterial host. Adsorptive membranes are reported to have been used to clarify, concentrate, fractionate and purify homogenized cell extract. Clarification has also been performed using hollow fibers and stacked membranes. Polymer rods have also been used for concentration, fractionation and purification.

6.2. Selective elution vs. differential migration

Membrane adsorbers can be operated in two distinct ways to separate and purify a designated biomolecule from similar contaminants. Often buffer conditions can be manipulated to instantaneously desorb, in series, a number of adsorbates. This procedure is referred to as selective elution. Considerations and advantages of selective elution are examined first. In other cases the desired product is gradually separated from contaminants due to its preferential affinity for

the stationary solid phase as the buffer conditions are kept constant, or gradually changed. This procedure, commonly called differential migration, will also be discussed.

Selective elution and differential migration represent the two extremes in operating adsorptive separations. Gradient elution of small molecules from granular columns often first results in differential migration, and then subsequently in selective elution as the concentration of the desorber increases. This "mixed-mode" scenario is less likely to occur in adsorptive-membrane separation of biomolecules, for reasons which we now address.

6.2.1. Selective elution

To date the most common application of adsorptive-membrane separation has been to concentrate product from dilute, clarified lysate or fermentation broth by pumping multiple bed volumes of feed through the membrane at buffered conditions which favor the adsorption of the desired product. After washing the bed to remove weakly-adsorbed contaminants, the product of interest and similar contaminants are eluted consecutively by changing the pH, ionic strength or organic composition of the mobile phase. Selective elution by isocratic, stepwise or gradient changes in mobile phase composition is commonly employed to purify the product. The membrane is regenerated and subsequently re-equilibrated in the adsorptive buffer in order to repeat the process.

Regeneration of adsorptive membranes, which are easily backflushed to remove residual protein contaminant, is determined by their chemistry. A strongly-basic QAE-ZetaPrep anion exchanger required only 1 *M* NaCl [54] for regeneration. Ion-exchange membranes can be completely regenerated by successively applying strong NaOH and HCl, or by in-line steam sterilization. Affinity columns, however, cannot be regenerated in this manner due to the labile nature of their ligands. By comparison, silica-based adsorbents dissolve within 30 min in boiling 1 *M* KOH (pH 14), as do analogues derived from magnesia and controlled-pore-glass [20].

As an example of concentration and purification by selective elution, immunoglobulin G (IgG) was adsorped from hybridoma culture supernatant onto a radial-flow membrane with an anion-exchange matrix in a running buffer of 50 m*M* Tris–HCl, pH 8.0 [54]. Weakly-bound contaminant proteins were seletively eluted by first increasing the NaCl concentration from 0 to 50 m*M* in the buffer. Another step increase of NaCl to 150 m*M* selectively eluted the IgG at a concentration ten times greater than that in the feed. Seventy percent of the original IgG was removed in the targeted fraction, while 30% of contaminating proteins were eliminated. The cartridge was regenerated with 1 *M* NaCl and re-equilibrated in the running buffer.

Elution by gradient or step-change in mobile phase composition often completely desorbs concentrated solutes. Such completely-desorbed solutes are convected toward the outlet of the adsorptive bed in the mobile-phase buffer at a velocity equal to that of the mobile phase. We noted in Section 5.3 that experimentally-obtained values of Z and log K for stacked-membrane adsorption have been found to be smaller than those for granular chromatographic beds operated under comparable conditions. This fact implies that relatively small changes in mobile phase composition can cause complete desorption of solutes from membrane matrices. It is therefore likely that separation by selective elution from adsorptive membranes is common, whether intended or not.

The thickness of the membrane bed in which separation takes place is relatively narrow. On the other hand, the entire length of the bed following desorption participates in mass transport processes explained in Section 5.2. During elution from adsorptive membranes, adjacent bands of solute broaden due to non-uniform flow, convective dispersion, and extracolumn backmixing. Completely-desorped solute bands broaden without further purification and can eventually overlap, producing a decrease in product purity relative to their initially desorbed state [66]. While non-uniform flow and extracolumn backmixing can severely increase peak broadening in membrane chromatography after desorption, these effects are not commonly predominant in granular packed beds. So packed-column length has less reported effect on res-

olution. Broadening during elution in granular columns is predominantly due to intraparticle diffusion. Provided flow non-uniformity and extracolumn mixing is limited, short membrane adsorbers are expected to degrade the purity of adjacent eluting bands less than longer granular columns.

As an example of lessened post-desorption broadening in membrane adsorbers, consider results from a separation by Tennikova and coworkers [38]. A negligible concentration gradient across one membrane was observed, resulting in instantaneous desorption throughout the adsorptive membrane bed. Resolution of model proteins on a GMA–EDMA 1-mm long membrane achieved by gradient elution were slightly better than those obtained using a packed, GMA–EDMA 140-mm long microcolumn [15]. It appears likely that this separation was achieved by selective elution. At a constant gradient slope in time, resolution in another membrane system was reported to be independent of flow-rate [14,42]. Resolution in this case was likely achieved by complete, selective elution of the solutes. Of course, performance of differing membrane adsorbers varies. Thicker beds have demonstrated relatively greater resolution by eliminating bypassing, improving flow uniformity [14].

6.2.2. Differential migration

Elution by gradient or step-change in mobile phase composition may also produce differential migration of concentrated solutes, in which the average velocity of each desorbed solute is proportional to its fractional equilibrium fluid-phase concentration. Resolution of adjacent bands in differential migration increases in proportion to the number of theoretical plates in a membrane. Differential migration further purifies a product from closely-related contaminants or a subtle variant.

Gradient elution is normally used to remove adsorbed components from membranes. Gradient elution is convenient since it is difficult to determine a priori the modifier concentration required to selectively elute just the desired species. In one example, a NaCl gradient removed human tumor necrosis factor, an unglycosylated polypeptide consisting of 157 amino acids, from an ion-exchange membrane [16]. Decreasing the gradient slope (or increasing the gradient volume) has been reported to improve resolution in stacked-membrane protein separations [11]. This feature can indicate separation by differential migration is taking place.

The additional effort required to determine appropriate step changes in mobile phase composition becomes more important at production scale, where efficient use of solvent and desorbent improves process economics. Stepwise elution typically produces more efficient membrane separations than linear gradients [14]. For example, stepwise NaCl increases eluted two plasma membrane glycoproteins from heparin and collagen stacked-membrane columns more successfully than a linear gradient [67]. In separate studies, stepwise salt increases eluted three model proteins from the respective membrane successively with less peak overlap and less solvent usage than a gradient [11,31]. High purity in consecutive step elutions, particularly at high protein loading, suggests binding sites available to biomolecules on adsorptive membranes are homogeneous.

Forethought in organizing a series of purification processes can also improve separation efficiency. A single elution step was used in each of a series of membrane adsorptions —cation-exchange, dye-affinity, and anion-exchange— to rapidly recover formate dehydrogenase [50]. The series was organized so that the elution buffer from one membrane served as the adsorption buffer for the next, avoiding buffer exchange, pH modification or dead time between successive steps.

The efficiency of selective elution using step changes in desorbent suggests this operating mode of membrane chromatography is preferable to differential migration, when conditions to effect selective elution can be determined.

6.3. Throughput of adsorptive membrane separations

The reported resolution, recovery and capacity of many adsorptive membranes are comparable to those of fixed-bed systems [16,56]. Pore size

apparently has little effect on resolution [30]. Relative concentration factors (about tenfold) and bed capacities of adsorptive membranes are smaller than those of packed-bed analogs [50,56].

The primary advantage of adsorptive membranes which compensates for these marginal characteristics is their substantially higher throughput. In one reported comparison, the total separation time using membranes was half that of corresponding fixed beds [16]. Another comparison reported that throughputs of cation- and anion-exchange membranes, 0.60 g/h of recombinant antithromin III and 2.1 g/h of MAb, respectively, were than four and thirteen times larger than with corresponding fixed-bed gel matrices [56]. Reported cycle times for membrane recovery were ten times faster than for columns [30]. The lack of mass transfer resistance by intraparticle diffusion permits greater interstitial velocities in membranes than in particulate beds while maintaining capacity [23]. This advantage has been referred to as "fast reaction kinetics" [14].

The speed at which membranes separations are performed decreases solvent usage and product degradation, which improves process economics and recovery yields. In mAb purification, for example, product losses by proteolytic cleavage or cleavage of disulfide bonds increase with processing time [54]. Radial membrane adsorption used to isolate mAb purified 10 l of supernatant within 3 h [54]. The recovery of β-1,4-D-xylanase with an SP-ZetaPrep 250 ion-exchange membrane yielded a higher product activity at less cost when compared with competitive ultrafiltration and precipitation processes [68]. The processing rate by ultrafiltration in this case was less than one third that of ion-exchange adsorption. Precipitation required uneconomical amounts of salts and solvents, while the costs of pumps and pumping were higher for ultrafiltration than for adsorption.

Neraly all reported analyses concur that backpressures in adsorptive membranes are low, even at high flow-rates [11,14,69]. Membrane backpressures are as much as 100 times lower than for comparable packed beds at the same flow-rate [15,38] (polymer rods are the single exception [18]). Owing to these limited backpressures, flow-rates of 200–500 ml/min are accessible without the use of high-pressure pumps or equipment [56,70]. Reduced backpressures become a greater advantage as the mobile phase viscosity and the scale of separation increase.

The porous nature and hydrophilicity of some membrane beds may account for additional reported advantages. Clogging by insoluble precipitates produced during adsorption or regeneration was reduced relative to packed beds [43]. Clogging could be prevented by prefiltering prior to adsorption. The use of detergents allows the separation of hydrophobic proteins and does not present difficulties [14]. The interstitial void volume due to empty spaces between spherical beads in a packed bed is avoided in membranes. This reduces the non-adsorptive dead volume by 26% [38]. Nominal values reported for bulk membrane bed porosity ranged from 50 to 82.7% [37,38]. Minimal shearing has also been noted [43].

6.4. Scale-up

Reports of scale-up of membrane chromatography to larger throughputs are favorable. A stacked-membrane column, scaled up by maintaining the bed length while increasing the bed diameter from 10 to 50 mm, produced a resolution equivalent to its laboratory-scale counterpart [14]. In another stacked-membrane scale-up resolution of monoclonal antibodies (mAb) was reproducible at 30 times the laboratory-scale flow-rate and sample volume [54]. The dynamic capacities of ion-exchange and dye-affinity membrane stacks for formate dehydrogenase remained constant after a 40-fold increase in cross-section [50].

A radial-flow membrane chromatographic column was scaled up by increasing both the diameter and height [13]. The flow-rate was increased in proportion to the cartridge volume in order to maintain the real-time behavior of the cartridge. The apparent specific capacity decreased slightly as the adsorptive bed volume increased to 12.8 times its original value.

There is, however, a dearth of commercially available production-scale devices whose characterization has been reported.

7. Applications of adsorptive membrane chromatography

In this section, reported applications of the adsorptive recovery of biomolecules using membrane substrates are reviewed. The applications are categorized according to the ligand chemistry of adsorption. We first consider affinity separations in Section 7.1. Examples of biospecific, dye ligand, immobilized metal, and pseudo-affinity adsorption have been reported. Ion-exchange membrane adsorption is summarized next in Section 7.2. Both weak and strong cation- and anion-exchange ligands are commercially available and have been examined. Section 6.3, considers membrane adsorption by Van der Waals or hydrophobic interaction. Membranes categorized as analogs of hydrophobic interaction and of reversed-phase chromatographic chemistries have had limited application. While indicating the range of applications of membrane adsorption in this section, we focus on applications to actual (rather than model) separations which suggest insights into the use of adsorptive membranes which could be extended by other members of the chromatographic community.

7.1. Affinity chromatography

Membranes were first widely used as substrates for affinity adsorption [11]. Development of an affinity system requires concerted effort focussed on achieving one-step purification of 1000-fold with nearly complete recovery in good scenarios. Membrane substrates offered a workable alternative to particulate affinity adsorbents whose low flow-rates were dictated by gel compressibility, pore diffusion and backpressure limitations [13]. Table 5 lists the ligand, ligate, elution conditions and geometry of several affinity membrane adsorptions. Some additional affinity separations are given in Table 3. A brief review of affinity applications can be found in Ref. [25]. We examine diffusional response, capacity, elution, and ligand choice in affinity membrane separations.

Table 5
Examples of affinity membrane adsorption

Ligand	Ligate	[22,69]
Protein A	γ Globulin	[39]
Ligand	Trypsin, trypsin-like proteases	[13]
Ligand	Glycoproteins	[67]
Heparin, collagen	Hydrophobic proteins	[14]
Dye	Bovine serum albumin (BSA)	[30]
Dye	Formate dehydrogenase, pyruvate decarboxylase	[30]
mAb	BSA	[71]
Protein A	IgG	[71]
Phe, Tyr	IgG, IgA	[22,69]
Copper	Amino acids	[23]

A brief order-of-magnitude anlysis illustrates the diffusional advantage of affinity membranes. The characteristic time for association between a ligand and an immobilized antigen is about 1 s, while the time for protein diffusion ($6 \cdot 10^{-7}$ cm^2/s for BSA) to the center of a 50-μm porous bead is greater than 40 s. So eliminating intraparticle diffusion increases the dynamic capacity and throughput efficiency of affinity adsorption (see Sections 5.2, 6.3) [39]. Improved throughputs were demonstrated using IgG adsorped to a Protein A hollow-fiber membrane [71] and amino acids separated by a metal affinity membrane (IMAM) [23].

Capacity of affinity membranes for biomolecules are in general lower than those observed in ion exchange or reversed-phase systems. An estimated one to two percent of potential affinity sites actually bind the ligate. Observed multipoint attachment of ligand and ligate also limits binding capacity [25]. Consequently, a capacity value of 1–2 mg/ml is acceptable. So demonstrated capacities listed in Table 3 for dye and pseudo-biospecific ligands which increase from 2.9 to 50.8 mg/ml are considered good. The open-pore structure of membrane matrices is reported to increase accessibility to affinity ligands and reduce steric hindrance relative to small-pore adsorbents.

Elution conditions required to remove ligates from affinity systems are determined by the interaction(s) involved. Ionic strength is increased to minimize non-specific electrostatic interactions and decreased to reduce hydrophic effects. Hydrophobic and Van der Waals interactions can also be absolved by reducing surface tension using a non-ionic detergent such as Triton X-100, ethylene glycol, or ethanol. High concentration of a chaotropic salt such as thiocyanate can eliminate both non-specific electrostatic and hydrophobic interactions. Elution from affinity membrane beds predominantly employs gradient or step changes in eluant composition to selectively elute products. Effluent curves measuring the adsorption, wash, and elution of a mixture of IgG and IgA on Phe and Tyr pseudo-affinity membranes have been reported [69].

Pseudo-biospecific ligands have been widely used in reported affinity-membrane adsorption. Examples include protein A, protein G, heparin, collagen, and two amino acids: arginine (Arg), and L-phenylalanine (Phe) coupled with an epoxide group. Josic and co-workers [14,67] reported pseudo-specific adsorption was preferable for preparative recovery since the mild elution conditions employed maintained the native conformation of glycoproteins. Antigen–antibody complexes created during indirect immunoaffinity adsorption were only disrupted by acid (pH 2.4) which resulted in a loss of enzymatic activity. Indirect immunoaffinity consists of a matrix coupled to protein A or G which non-covalently binds antibody. The antibody then, in turn, associates with the antigen. It was also observed that monoclonal antibodies (mAb) raised against membrane glycoproteins lost almost 90% of their binding activity upon covalent immobilization [67].

Dye adsorbents which demonstrate affinity for nucleotide binding sites on enzymes have also been employed. Monoclonal antibodies were the most common immunoaffinity ligand used. An immobilized metal affinity membrane (IMAM) was developed by chemical conversion of the membrane epoxide to iminodiacetate and subsequent chelation with copper [23]. Affinity ligands are covalently attached to membrane matrices using coupling chemistries briefly reviewed in Section 4.2. Stable linkages are necessary to prohibit leaching of the ligand into the effluent stream. The length of spacer armed used is critical in the observed performance of affinity membrane systems.

7.2. Ion-exchange separations

Ion-exchange separations take advantage of electrostatic interaction between surface charges on biomolecules such as amino acids or proteins and clusters of charged groups on membrane. An adsorbing biomolecule displaces counterions associated with the surface, discharging a complementary buffer salt in the process. Adequate buffering is required to shield native protein structures from changes in pH adjacent to exchange surfaces (Donnan effect) and pH effects induced by sorption. Selection of an appropriate buffer is critical to the success of membrane ion-exchange. Large molecules ($M_r > 1\,000\,000$) such as plasmid DNA, are able to access charged groups which envelope large pores of membrane adsorbers, though they would commonly be excluded from cellulose-based ion exchangers. Mobile phases and buffers employed in ion-exchange bioseparations are non-denaturing to hydrophilic proteins. Elution and recovery of biologicals using ion exchange are considered, as well as effects of additivese and flowrate on performance.

Table 6 lists reported ion-exchange membrane adsorption of a number of proteins, polypeptides and nucleic acids. A brief summary of ion-exchange membrane applications may also be found in [25]. Purification factors achieved by ion exchange are typically an order of magnitude lower than immunoaffinity or dye affinity adsorption. On the other hand, lack of leaching from the adsorbent, less inactivation during adsorption and reduced expense for ligand favor ion exchange.

Ion-exchange membrane separations are most often accomplished by selectively eluting (see Section 6.2) the desired product using an increase in salt to reduce the retention factor. Separation by differential migration is less com-

Table 6
Examples of ion-exchange membrane adsorption

Ligand	Ligate	Geometry	Ref.
Q	Polypeptide TNF	Membrane stack	[16]
PEI	BSA, Lys, Ova	Formed in place	[19]
SP	TPA	Zetaprep	[72]
S.Q	Formate dehydrogenase	Stack	[50]
	Membrane proteins		[14]
QAE	mAb	Zetaprep	[54]
SP	β-1,4-D--Xylanase	Zetaprep	[68]
	Nucleic acid		[43]
Q, S	Antithrombin III, mAb	Stack	[55,56]

mon. Thermodynamic functions of ionic strength in membranes such as capacity, equilibrium, selectivity, and retention were considered in Section 5.3. Alternatively, elution by adjusting pH can permit consecutive ion-exchange adsorptions without intervening buffer exchange. One novel ion-exchange application produced sequential elution of denatured proteins, (oligo)ribonucleotides, DNA and DNA complexes using organic eluants at high ionic strength [43].

The hydrophilicity of adsorptive membrane matrices and the biofavorable eluting conditions possible in ion-exchange desorption result in high reported recoveries. Separation of rat-serum and kidney-plasma membrane proteins by anion exchange gave recoveries exceeding 85% [14]. BSA recovery from an S cation-exchange membrane was better than 80% [42]. Recovery of monoclonal antibodies from cell culture supernatant using anion exchange were 96% [55].

Ion exchange is often used as the first concentrating step following clarification of a cell extract (See Section 6.1). Effects of components which remain in the clarified cell supernatant from typical lysis buffers such as detergents have been examined. Non-ionic and zwitterionic detergents had no adverse effect on membrane anion-exchange separations at concentrations up to 1% [14], even though clouding in high-salt solutions above critical micelle concentration interfered with optical detection. Anionic SDS prohibited separation by binding to proteins, coating them with negative charges. Reported scale-up to preparative throughputs is most commonly performed using ion-exchange systems (See Section 6.3) since concentration by ion exchange is widely employed. For example, isolation of mAb with p*I* values between 5.4 and 6.1 from hybridoma culture supernatant employed anion-exchange QAE cartridges at laboratory, preparative and pilot scales [54].

Of course, operating conditions significantly influence outcomes of membrane ion exchange, as discussed in Sections 5 and 6. Peak-shapes resulting from ion exchange have been improved by modifying commercially available membrane adsorbers to reduce extracolumn volume [42]. Gradient changes in salt concentration were replaced by steps to desorb proteins, improving resolution. However flow-rate had an undetectable effect on peak shape, indicating the on–off nature typical of membrane ion-exchange separation of proteins.

7.3. Hydrophobic and reversed-phase separations

Separations of biomolecules on hydrophobic and reversed-phase stationary phases rely on Van der Waals interactions between uncharged patches on the molecules and water-heating surfaces of the adsorbent. Selection of an appropriate buffer and elution conditions is critical to ensure useful isoforms of the product can be obtained from the separation. The tendency of hydrophobic interactions is to denature proteins. For example, only 20% of original tumor necrosis factor was recovered in biologically-active form from a C-4 membrane adsorber [16], due to partial dissociation of active trimer into inactive monomers. Acetic acid rinsing was necessary to remove remaining inactivated monomer from the matrix.

Reported hydrophobic separations listed in Table 7 are useful for comparison with packed-column results. They may also indicate poten-

Table 7
Examples of hydrophobic membrane adsorption

Ligand	Ligate	Geometry	Ref.
C_4	Human tumor necrosis factor	Membrane stack	[16]
C_4, C_8	Myo, Lys, Ova, Chy	Membrane stack	[38]
STDVB	[D-Phe]-bradykinin, egg albumin, HSA	Polymer rod	[11,18]
GMA–EDMA	Myo, Lys, Rib, Chy	Membrane disk	[11]

tially useful assays with which to monitor protein-purification sequences.

Protein capacities available on hydrophobic membrane adsorbers shown in Table 3 are typical of packed-bed values: 10–100 mg/ml stationary phase. Adsorption in these systems occurs at high salt. So hydrophobic interaction may be performed immediately after ion-exchange concentration without an intermediate buffer exchange. The membrane both desalts the feed and discriminates between molecules of differing hydrophobicity.

Elution from hydrophobic adsorbents can be effected by lowering temperature, changing pH, or adding polyol such as ethylene glycol or non-ionic detergent to the carrying buffer. Most commonly, composition of an organic modifier is increased in quantity sufficient to desorb the product of interest without precipitating it within the system. In reported examples, retention factor decreased rapidly with small changes in mobile-phase acetonitrile composition [18]. This allowed peptide separation on hydrophobic membranes to occur ten times as fast as on beaded styrenic resin. The sum of natural logs of the retention and capacity factors on reversed-phase polymer rods were observed to decrease in proportion to the organic volume fraction [18]. This performance is comparable to reported reversed-phase packed-bed behavior.

Relatively few hydrophobic or reversed-phase membrane adsorptions of biomolecules have been performed, due to the hydrophilic nature of the most labile proteins and polypeptides. Hydrophobic membrane adsorbers are commercially available in more limited varieties than their ion-exchange or affinity counterparts.

8. Conclusions

Adsorptive membranes are available in a variety of chemistries which are largely hydrophilic with minimal secondary interactions. Owing to the small bed heights, large cross-sectional surface areas and neglible intraparticle diffusion common to most adsorptive membranes, they exhibit low backpressures, short residence times and high volumetric throughputs. These features increase throughput and decrease processing times, relative to conventional fixed beds, reducing the requirement for expensive or hazardous solvents and tankage. Their shorter residence times reduce protein degradation by proteolysis and denaturation.

The range of geometries available for membrane adsorption allow incorporation of these systems into early-stage product concentration and recovery from cell lysate. Different models with more theoretical plates are available to fractionate and purify the desire product from closely related contaminants.

The separation performance of existing adsorptive membranes is reported to rival that of packed chromatographic beds in many cases. However, a number of anomalous mass transport effects have been observed: non-uniform flow, dead spaces and extra-column dispersion. These effects are not observed in all membrane systems and appear to be eliminated by proper design. Their combined effect where present is to reduce adsorptive membrane efficiency on the laboratory scale, as measured by the plate height, to the level of packed beds. Theory indicates that adsorptive membrane efficiencies should exceed those of granular beds by a factor

of ten or more. Although acceptable for small-scale analysis, adsorptive membranes appear to be capable of substantial improvement.

Future applications of adsorptive membranes will take advantage of their demonstrated strengths. Speed and resolution make membrane chromatography a likely candidate for on-line process monitoring and sidestream analysis. Low backpressure and low volumetric capacity relative to packed beds suggest that adsorptive membranes may be useful as subunits in simulated moving beds. Cross-flow adsorptive membrane geometries would allow product recovery from crude homogenates and unclarified cell culture supernatants without fouling of the membrane.

References

[1] W.H. Hancock, S. Wu and J. Frenz, *LC · GC*, 10 (1992) 96–104.

[2] X. Zhang, R.D. Whitley and N.-H.L. Wang, presented at *the AIChE Annual Meeting, Los Angeles, CA, November 17–22, 1991.*

[3] V.R. Anicetti, B.A. Keyt and W.S. Hancock, *Tibtech*, 7 (1989) 342–349.

[4] R.C. Dean, presented at *the Am. Soc. Mech. Eng. Seminar on Process Equipment Technology for the Manufacture of Biopharmaceuticals, 1988.*

[5] K.L. Carson, *GEN*, 14, No. 6 (1994) 12.

[6] J.A. Asenjo, J. Parrado and B.A. Andrews, *Ann. N.Y. Acad. Sci.*, 646 (1991) 334–356.

[7] M.D. Weiss, *GEN*, 14, No. 7 (1994) 8.

[8] A. Sadana, *BioPharm.* 7, No. 3 (1994) 34.

[9] T.G.I. Ling and B. Mattiasson, *Biotechnol. Bioeng.*, 34 (1989) 1321–1325.

[10] E. Klein, *Affinity Membranes. J. Wiley, New York*, 1991, p. 14.

[11] T.B. Tennikova and F. Svec, *J. Chromatogr.*, 646 (1993) 279–288.

[12] J.G. Dorsey, W.T. Cooper, J.F. Wheeler, H.G. Barth and J.P. Foley, *Anal. Chem.*, 66 (1994) 500R–546R.

[13] S.H. Huang, S. Roy, K.C. Hou and G.T. Tsao, *Biotechnol. Prog.*, 4 (1988) 159–165.

[14] D. Josic, J. Reusch, K. Loster, O. Baum and W. Reutter, *J. Chromatogr.*, 590 (1992) 59–76.

[15] T.B. Tennikova, B.G. Belenkii and F. Svec, *J. Liq. Chromatogr.*, 13 (1990) 63–70.

[16] J. Luksa, V. Menart, S. Milicic, B. Kus, V. Gaberc-Porekar and D. Josic, *J. Chromatogr. A* 661 (1994) 161–168.

[17] Q.C. Wang, F. Svec and J.M.J. Frechet, *Anal. Chem.*, 65 (1993) 2243–2248.

[18] Q.C. Wang, F. Svec and J.M.J. Frechet, *J. Chromatogr. A*, 669 (1994) 230–235.

[19] Y. Li and H.G. Spencer, *J. Biotechnol.*, 26 (1992) 203–211.

[20] R.M. Chicz, Z. Shi and F.E. Regnier, *J. Chromatogr.*, 359 (1986) 121–130.

[21] M. Kim, J. Kojima, K. Saito and S. Furusaki, *Biotechnol. Prog.*, 10 (1994) 114–120.

[22] M. Kim, K. Saito, S. Furusaki, T. Sugo and I. Ishigaki, *J. Chromatogr.*, 586 (1991) 27–33.

[23] H. Iwata, K. Saito and S. Furasaki, *Biotechnol. Prog.*, 17 (1991) 412–418.

[24] G.C. Serafica, J. Pimbley and G. Belfort, *Biotechnol. Bioeng.*, 43 (1994) 21–36.

[25] P. Langlotz and K.H. Kroner, *J. Chromatogr.*, 591 (1992) 107–113.

[26] R.S. Tutunjian, *Bio/Technol.*, 3 (1985) 1985 615–626.

[27] R. Molinari, J.L. Torres, A.S. Michaels, P.K. Kilpatrick and R.G. Carbonell, *Biotechnol. Bioeng.*, 36 (1990) 572–580.

[28] S.-Y. Suen and M.R. Etzel, *Chem. Eng. Sci.*, 47 (1992) 1355–1364.

[29] G.B. Cox, *LC · GC*, 8 (1990) 690–694.

[30] K.-G. Briefs and M.-R. Kula, *Chem. Eng. Sci.*, 47 (1992) 141–149.

[31] J.A. Gerstner, R. Hamilton and S.J. Cramer, *J. Chromatogr.*, 596 (1992) 173–180.

[32] R. Hamiltonian, presented at *the AIChE Annual Meeting, Los Angeles, CA, November 17–22, 1991.*

[33] D.K. Roper and E.N. Lightfoot, presented at *the AIChE Annual Meeting, St. Louis, MO, November 7–12, 1993.*

[34] G. Guillot, in E. Guyen, J.P. Nadal and Y. Pomeau (Editors), *Disorder and Mixing*, Kluwer, New York, 1988.

[35] S. Saini and J.T. Ferrucci, in D.P. Swanson, H.M. Chilton and J.H. Thrall (Editors), *Pharmaceuticals in Medical Imaging*, Macmillan, New York, 1990.

[36] D.K. Roper, M.E. Anderson and E.N. Lightfoot, in preparation.

[37] M.S. Le and J.L. Sanderson, US Pat., 4 895 806 (1990).

[38] T.B. Tennikova, M. Bleha, F. Svec, T.V. Almazova and B.G. Belenkii, *J. Chromatogr.*, 555 (1991) 9–107.

[39] M. Unarska, P.A. Davies, M.P. Esnouf and B.J. Bellhouse, *J. Chromatogr.*, 519 (1991) 53–67.

[40] D.K. Roper, *Ph.D. Thesis*, University of Wisconsin–Madison, Madison, WI, 1994.

[41] R.B. Bird, W.E. Stewart and E.N. Lightfoot, *Transport Phenomena*, Wiley, New York, 1960.

[42] O.W. Reif and R. Freitag, *J. Chromatogr. A*, 654 (1993) 29–41.

[43] N. van Huynh, J.C. Motte, J.F. Pilette, M. Decleire and C. Colson, *Anal. Biochem.*, 211 (1993) 61–65.

[44] K.K. Raths, *M.S. Thesis*, University of Wisconsin–Madison, Madison, WI, 1992.

[45] M.A. Northrup, T.J. Kulp, S.M. Angel and G.F. Pinder, *Chem. Eng. Sci.*, 48 (1993) 13–23.
[46] D.L. Koch and J.F. Brady, *J. Fluid Mech.*, 154 (1985) 399–427.
[47] D.K. Roper and E.N. Lightfoot, *J. Chromatogr.*, in press.
[48] N.B. Afeyan, N.F. Gordon, L. Mazsaroff, L. Varady, S.P. Fulton, Y.B. Yang and F.E. Regnier, *J. Chromatogr.*, 519 (1990) 1–29.
[49] F.H. Arnold, H.W. Blanch and C.R. Wilke, *Chem. Eng. J.*, 30 (1985) B9–B23.
[50] B. Champluvier and M.-R. Kula, *Bioseparation*, 2 (1992) 343–351.
[51] S.-Y. Suen, *Ph.D. Thesis*, University of Wisconsin-Madison, Madison, WI, 1994.
[52] D.D. Frey, R. Van de Water and B. Zhang, *J. Chromatogr.*, 597 (1992) 173–179.
[53] S. Krause, K.H. Kroner and W.-D. Deckwer, *Biotechnol. Techn.*, 5 (1991) 199–204.
[54] A. Jungbauer, F. Unterluggauer, K. Uhl, A. Buchacher, F. Steindl, D. Pettauer and E. Wenisch., *Biotechnol. Bioeng.*, 32 (1988) 326–333.
[55] D. Lutkemeyer, S. Siwiora, H. Buntemeyer and J. Lehmann, presented at *the 10th DECHEMA Annual Biotechnology Meeting, Karlsruhe, 1–3 June, 1992.*
[56] D. Lutkemeyer, M. Bretschneider, H. Buntemeyer and J. Lehmann, *J. Chromatogr.*, 639 (1993) 57–66.
[57] B. Champluvier and M.-R. Kula, *J. Chromatogr.*, 539 (1991) 315–325.
[58] W.F. Weinbrenner and M.R. Etzel, *J. Chromatogr. A*, 662 (1994) 414–419.
[59] S.-Y. Suen, M. Caracotsios and M.R. Etzel, *Chem. Eng. Sci.*, 48 (1993) 1801–1812.
[60] S. Yamamoto and Y. Sano, *J. Chromatogr.*, 597 (1992) 173–179.
[61] J.L. Coffman, D.K. Roper and E.N. Lightfoot, *Bioseparation*, 4 (1994) 183–200.
[62] R. Scopes, *Protein Purification*, Springer, New York, 1987.
[63] E.N. Lightfoot and M.C.M. Cockrem, *Sep. Sci. Technol.*, 22 (1987) 165–189.
[64] S. Englard and S. Seifter, in M.P. Deutscher (Editor), *Methods in Enzymology* Vol. 182, Academic Press, San Diego, 1990.
[65] P. Schadle, presented at *PrepTech94, Industrial Separations Technology Conference Secaucus, NJ, March 22–24, 1994.*
[66] B.G. Belinki, A.M. Podkladenko, O.I. Kurenbin, V.G. Mal'tsev, D.G. Nasledov and S.A. Trushin, *J. Chromatogr.*, 645 (1993) 10–15.
[67] D. Josic, K. Zeilinger, Y.-P. Lim, M. Raps, W. Hofmann and W. Reutter, *J. Chromatogr.*, 484 (1989) 327–335.
[68] L.U.L. Tan, E.K.C. Yu, G.W. Louis-Seize and J.N. Saddler, *Biotechnol. Bioeng.*, 30 (1987) 96–100.
[69] M. Kim, K. Saito, S. Furusaki, T. Sato, T. Sugo and I. Ishigaki., *J. Chromatogr.*, 585 (1991) 45–51.
[70] K.C. Hou and T.-P.D. Liao, *US Pat.*, 4 663 163 (1987).
[71] S. Brandt, R.A. Goffe, S.B. Kessler, J.L. O'Connor and S.E. Zale, *Bio-Technol.*, 6 (1988) 779–782.
[72] A. Upshall, A.A. Kumar, M.C. Bailey, M.D. Parker, M.A. Favreau, K.P. Lewison, M.L. Joseph, J.M. Maraganore and G.L. McKnight, *Bio/Technol.*, 5 (1987) 1301–1304.
[73] K.C. Hou and G. Cogswell, *US Pat.*, 4 639 513 (1987).